MECHANISM OF REDUCTION OF CYMANTRENE (TRICARBONYL η^5-CYCLOPENTADIENYLMANGANESE) AND ITS METHYL CARBOXIMIDATE DERIVATIVE

Michèle SALMAIN[a1], Gérard JAOUEN[a2], Jan FIEDLER[b1], Romana SOKOLOVÁ[b2] and Lubomír POSPÍŠIL[b3,*]

[a] *Ecole Nationale Supérieure de Chimie de Paris, Laboratoire de Chimie Organométallique (UMR CNRS 7576), 11 rue Pierre et Marie Curie, 75231 Paris Cédex 05, France; e-mail: [1] salmain@ext.jussieu.fr, [2] jaouen@ext.jussieu.fr*

[b] *J. Heyrovský Institute of Physical Chemistry, Academy of Sciences of the Czech Republic, Dolejškova 3, 182 23 Prague 8, Czech Republic; e-mail: [1] jan.fiedler@jh-inst.cas.cz, [2] sokolova@jh-inst.cas.cz, [3] lubomir.pospisil@jh-inst.cas.cz*

Received October 4, 2000
Accepted December 12, 2000

Dedicated to the memory of the late Professor Antonín A. Vlček.

The mechanisms of electrochemical reduction of cymantrene, $[Mn(CO)_3(\eta^5\text{-}Cp)]$, and its ring-substituted methyl carboximidate derivative, $[Mn(CO)_3(\eta^5\text{-}C_5H_4C(NH)OMe)]$, were studied by voltammetry, *in situ* IR spectroelectrochemistry and preparative electrolysis. The product of one-electron reduction undergoes further chemical reactions. Comparison of the data obtained under atmosphere of argon and that of carbon monoxide leads to the conclusion that a ligand substitution reaction and dimerization participate in the overall reaction sequence. FTIR spectra recorded *in situ* suggest product dimerization, the formation of $[Mn(CO)_5]^-$ and, to a lesser extent, other unstable species. The dimer formation was not observed in the course of the reduction of the carboximidate.

Keywords: Cymantrene; Manganese tricarbonyl complexes; Electroreductions; Imidates; Cyclopentadienyl ligands; Spectroelectrochemistry; Voltammetry.

Reactions of transition metal carbonyl complexes have been studied mainly in relation with their properties to catalyze hydroformylation, carbonylation, polymerization and many other oxo-processes[1]. Before the substrate can coordinate to a catalyst, a vacant site must be available on the central atom of the complex. This can be achieved by changing the stable 18-electron configuration of the complex. Reduction and oxidation reactions play a key role in the labilization of the coordination sphere that finally results in the ligand substitution. Substitution processes proceed

mainly through dissociative pathways in which the bond of the departing ligand is broken before the incoming ligand coordinates to the metal[2]. Associative pathways are seldom encountered, only for complexes capable of delocalizing an electron pair over one of its ligands[3]. In both cases, the overall electron transfer reaction involves short-lived intermediates that are often difficult to identify. Redox cross-reactions between intermediates generated at the electrode surface and the parent complex in the solution often cause catalytic chain reactions[4–8]. The work reported herein deals with the electrochemical reduction of the two tricarbonylmanganese complexes **1** and **2** depicted in Scheme 1.

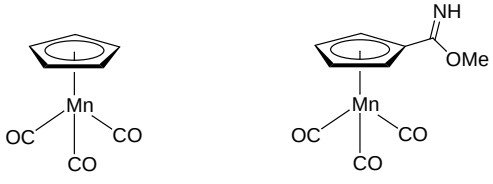

1 **2**

SCHEME 1

Complex **2** is of particular importance, since it is water-soluble and its methyl carboximidate group can be coupled readily with the ε-amino group of lysine residues of peptides or proteins. Hence, compound **2** is a good candidate for the carbonyl metallo immunoassay (CMIA), recently introduced by Jaouen *et al.*[9–11]. The CMIA makes use of the intense and specific CO stretching vibration bands in the IR spectrum of transition metal carbonyl complexes for the immunoanalytical determination of molecules, used in clinical practice. An alternative detection method could take advantage of the electroactivity of the metallo-organic label, with the perspective of a low detection limit achieved by adsorptive accumulation on electrodes[12]. The objective of this work is to elucidate redox properties of the precursor compound **1** and the marker **2** in non-aqueous medium. Clarification of the mechanism is desirable prior to the application of electrochemical methods to labelled protein systems. The electron transfer processes of complex **1** have been reported several times[13–17], most recently by Sawtelle *et al.*[18]. However, reaction pathways and intermediates have not been fully identified. Sawtelle *et al.*[18] interpreted the irreversibility of the reduction of **1** as an EC process (electron transfer followed by a chemical reaction) in which cyclopentadienyl ring slippage leads to the formation of a dinuclear complex. We present here data and arguments proving the partic-

ipation of yet other consecutive chemical reactions in the overall reaction mechanism.

EXPERIMENTAL

Chemicals

Cymantrene (**1**) was purchased from Aldrich and used as received. Complex $[Mn(CO)_3(\eta^5\text{-}C_5H_4C(NH)OMe)]$ (**2**) was synthesized from **1** according to a procedure similar to the preparation of $[Cr(CO)_2(NO)(\eta^5\text{-}C_5H_4C(NH)OMe)]$ (ref.[19]). Tetrabutylammonium hexafluorophosphate ($TBAPF_6$), used as supporting electrolyte, was recrystallized and dried in an oven. Acetonitrile was purified by reflux with CaH_2 and distilled prior to use.

Electrochemical Procedures

Electrochemical measurements were done using a laboratory-built electrochemical system consisting of a fast-rise-time potentiostat and an interface to a personal computer *via* an AD/DA card, PcLab model PCL818 (Advantec Co.). Exhaustive electrolysis was performed using an EG&G potentiostat, Model 273A. A three-electrode electrochemical cell was used with the Ag|AgCl|1 M LiCl reference electrode separated from the test solution by a salt bridge. The working electrode was a valve-operating static mercury electrode, model SMDE2 (Laboratorní Přístroje, Prague). The voltage scan rate was synchronized with the formation of a fresh mercury drop. The auxiliary electrode was cylindrical platinum minigrid. Oxygen was removed from the solution by passing a stream of argon. Experiments were performed at 20 °C. Electrochemical measurements under CO atmosphere were performed by passing a stream of gaseous CO (Linde) purified with aqueous KOH, followed by a column filled with molecular sieves. The oxidation potential of ferrocene measured against our reference electrode was +0.52 V. The cyclic staircase voltammetry was applied in its standard mode using a triangular voltage waveform and scan rates from 0.5 to 130 V s^{-1}. The other type of voltammetric measurement used a trapezoidal voltage shape. In this mode, the electrode potential was scanned to a selected value where the potential was held for 20 s ± 0.5 ms. *In situ* IR spectroelectrochemical measurements were performed using an optically transparent thin-layer cell with a platinum minigrid as a working electrode in a three-electrode arrangement. IR spectra were recorded on a Philips PU9800 FTIR spectrometer.

RESULTS AND DISCUSSION

Reduction of Cymantrene **1**

Typical cyclic voltammetric responses of **1** in acetonitrile are summarized in Fig. 1.

Complex **1** exhibits a seemingly simple voltammetric picture: irreversible reduction peak A and small anodic waves B′, C′ and D′ at –1.49, –1.14 and –0.11 V, respectively (see Table I). Anodic counterpart of peak A was not observed, neither at high scan rates nor at –35 °C. The position and the char-

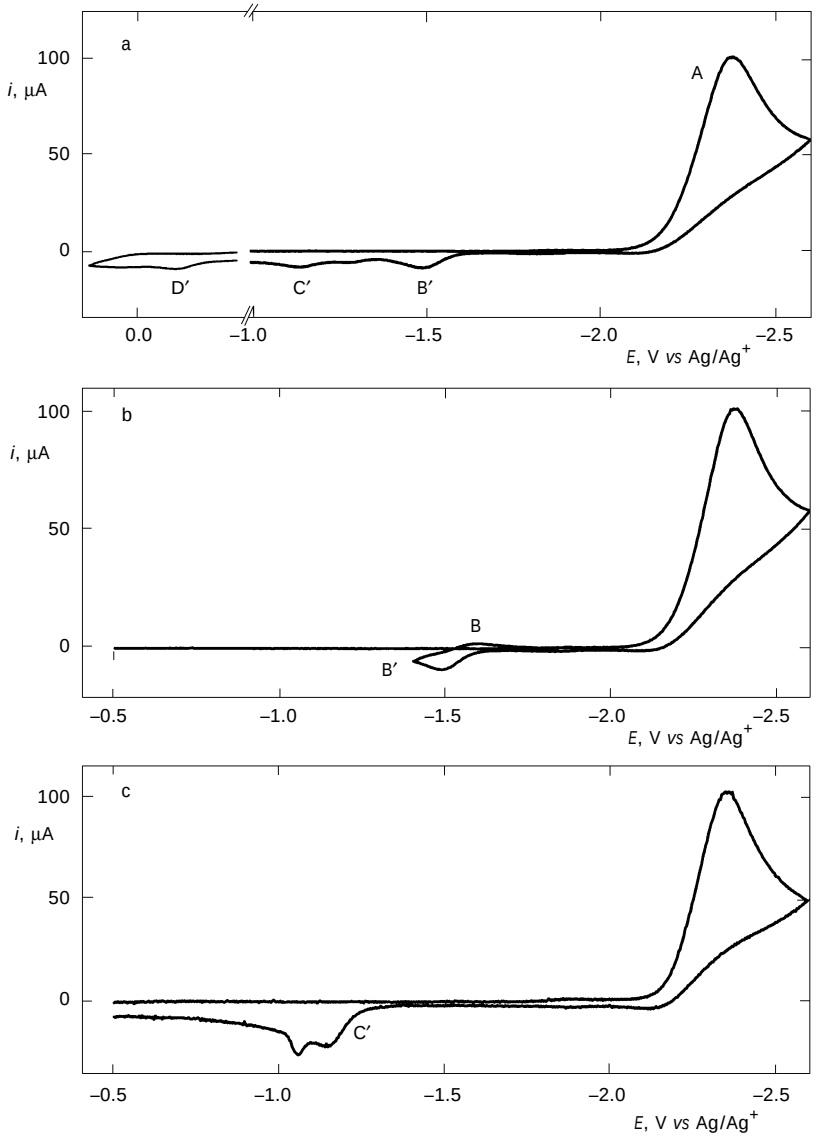

FIG. 1

Cyclic voltammetry of 2.6 mM $[Mn(CO)_3(\eta^5\text{-Cp})]$ (**1**) and 0.1 M $TBAPF_6$ in acetonitrile at the scan rate 0.5 V s^{-1}: potential scan beginning and ending at 0 V (a), scan with the second vertex potential set at –1.4 V (b), voltammetry under CO atmosphere (c)

acter of the main, likely one-electron reduction peak A at –2.38 V, are in agreement with previously published data[18]. The uptake of one electron follows from comparison of the voltammetric peak current with that of ferrocene. However, the exhaustive electrolysis (see below) requires about two electrons per molecule before the faradaic current decays to the level of the background current.

The reduction of **1** was further monitored by *in situ* IR spectroelectrochemistry, using an optically transparent platinum electrode. The two absorption bands at 2 021 and 1 933 cm^{-1}, assigned to the three coordinated carbonyl ligands and characteristic of the C_{3v} symmetry of **1**, gradually disappear when the potential reaches values more negative than –2.2 V, corresponding to the onset of voltammetric peak A (Fig. 2).

Two new pairs of bands between 1 700 and 1 900 cm^{-1} and two weak bands around 1 600 cm^{-1} (Table II) progressively arise. Reverse sweeping to the potential of peak C′ restores the bands of the starting material to approximately 50% of the original intensity, whereas the bands at 1 776 and 1 731 cm^{-1} disappear. Persistence of the bands at 1 898 and 1 865 cm^{-1} suggests the presence of product(s) formed by an irreversible chemical reaction.

Voltammetric and spectroelectrochemical results indicate that the primary product of the one-electron reduction is highly unstable and undergoes a rapid decomposition. The lost of one CO ligand and the subsequent

TABLE I
Potentials (in V) of assigned voltammetric peaks in the cyclic voltammograms of **1** and **2**, referred to Ag|1 M AgCl electrode[a] in acetonitrile at v = 0.5 V s^{-1}

Peak	**1**[b]	**1**[c]	**2**[b]	**2**[c]
A	–2.38	–2.35	–2.09	–2.07
A′	–	–	–1.94	–1.92
B	–1.57	–	–1.86	–1.85
B′	–1.49	–	–1.76	–1.75
C′	–1.14	–1.15	–	–1.12
D′	–0.11	–0.11	–0.09	–0.10
S	–	–	–2.65	–2.65

[a] Observed: $E_{1/2}(Fc/Fc^+)$ = +0.52 V. [b] Under an Ar atmosphere. [c] Under a CO atmosphere; CO-saturated solution.

coordination of a solvent molecule (abbreviated Solv in Eq. (*1*)) is a process participating in the reaction sequence[20]. Such reaction was observed also during photolysis of **1**.

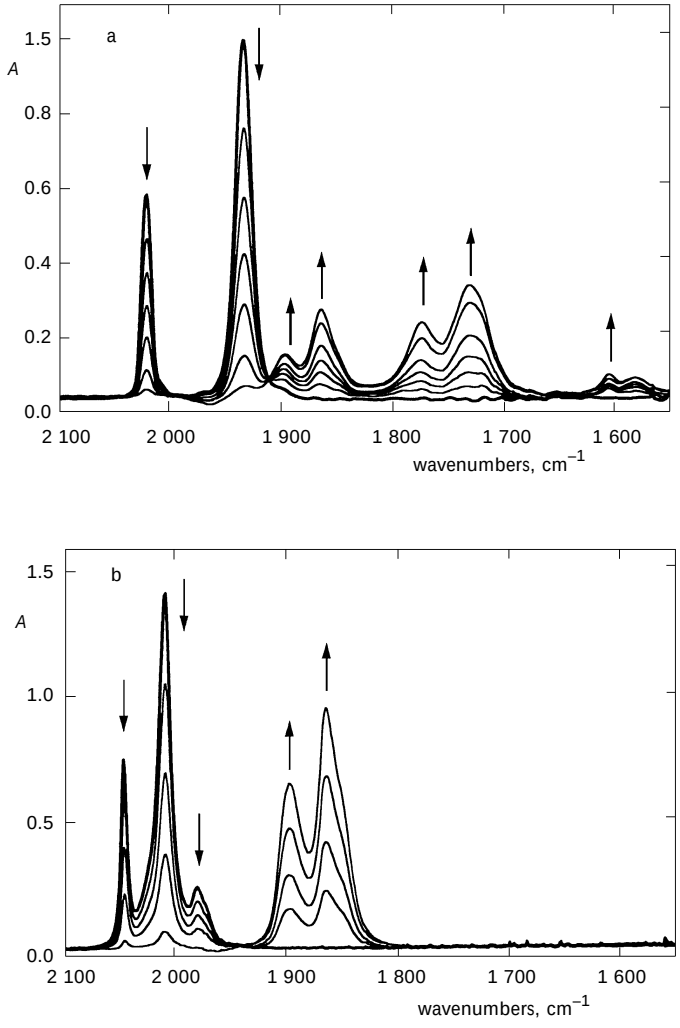

FIG. 2

FTIR spectroelectrochemistry of 5 mM $[Mn(CO)_3(\eta^5\text{-Cp})]$ (**1**) and 0.1 M $TBAPF_6$ in acetonitrile; spectra correspond to potentials –1.40, –2.25, –2.27, –2.29, –2.31, –2.37 and –2.41 V (a). FTIR spectroelectrochemistry of 7 mM $[Mn_2(CO)_{10}]$ and 0.1 M $TBAPF_6$ in acetonitrile; spectra correspond to potentials –1.00, –1.30, –1.45, –1.60 and –1.75 V (b)

$$[Mn(CO)_3(\eta^5\text{-Cp})] + e \Rightarrow [Mn(CO)_3(\eta^5\text{-Cp})]^- \xrightarrow{-CO} \quad (1)$$
1 **1**$^-$

$$[Mn(CO)_2(\eta^5\text{-Cp})]^- \xrightarrow{Solv} [Mn(CO)_2(Solv)(\eta^5\text{-Cp})]^-$$
3$^-$ **4**$^-$

Only the anodic peak B′ has its cathodic counterpart, peak B, at –1.57 V. The peak B appears in the second cathodic voltage scan. It therefore corresponds to an intermediate formed by the electron transfer reaction. The redox pair B/B′ is a chemically reversible system, as follows from voltammogram in Fig. 1b. Voltammetry with a trapezoidal potential shape and accumulation at –2.6 V shows an increase in peaks B′ and C′, whereas the accumulation at –1.4 V (prior to the second voltammetric cycle) completely eliminates peak B. This confirms that the generated redox pair B/B′ corresponds to a newly formed species and we interpret it as the **4**$^-$/**4** couple. Another strong argument for the assignment of the voltammetric peaks at

TABLE II
IR ν(CO) bands for **1**, **2** and related manganese complexes that are relevant to this study

Compound	ν(CO) (observed)	Compound	ν(CO) (reported)
1	2 021, 1 933	$[Mn(CO)_3(Cp)]$	2 021, 1 932[b]
Reduced **1**	1 898, 1 865	$[Mn(CO)_5]^-$	1 895, 1 855[c]
		$[Mn(CO)_2(H)(Cp)]^-$	1 860[c]
	[a]	$[Mn_2(CO)_5(Cp)_2]^-$	
	1 776	$[Mn_2(CO)_6(Cp)_2]^{2-}$	
		$[Mn(CO)_2(H)(Cp)]^-$	1 770[d]
	1 731	$[Mn_2(CO)_6(Cp)_2]^{2-}$	
	[a]	$[Mn(CO)_2(Cp)]^{2-}$	1 685, 1 600, 1 550[d]
	1 605	$[Mn(CO)_2(CHO)(Cp)]$	
	1 587	$[Mn_2(CO)_5(Cp)_2]^{2-}$	
2	2 025, 1 941, 1 653	$[Mn(CO)_3(C_5H_4C(NH)OMe)]$	
Reduced **2**	1 936, 1 850, 1 610	$[Mn(CO)_2(C_5H_4C(NH)OMe)]^-$	

[a] Not observed or overlapped by bands of predominant species, [b] Ref.[20], [c] Ref.[16], [d] Ref.[15]

–1.50 V to the $\mathbf{4}^{-}/\mathbf{4}$ couple comes from the dissappearence of voltammetric peak B′ when the ligand dissociation equilibrium is suppressed by saturating the solution with gaseous CO (Fig. 1c). The effect of CO on voltammetry of **1** was reversible in the sense that subsequent prolonged passing of argon through the solution restored the curve in Fig. 1a. The limited stability of these species is caused by facile substitution reactions[21] of the CO ligand and the coordinated solvent.

Chemical reduction of pyridine substituted derivative[15] $[Mn(CO)_2(\eta^5\text{-}Cp)(py)]$ leads to dication that may further add a proton and form a hydride (Eq. (*2*)).

$$\underset{\mathbf{3}^{-}}{[Mn(CO)_2(\eta^5\text{-}Cp)]^{-}} + e \Rightarrow \underset{\mathbf{3}^{2-}}{[Mn(CO)_2(\eta^5\text{-}Cp)]^{2-}} \xrightarrow{+\ H^{+}} \underset{\mathbf{5}^{-}}{[Mn(CO)_2(H)(\eta^5\text{-}Cp)]^{-}} \qquad (2)$$

Participation of an analogous process can increase the charge consumption observed during the exhaustive electrolysis. However, intense ν(CO) bands of $\mathbf{3}^{2-}$ reported[15] at 1 685, 1 600 and 1 550 cm^{-1} are not observed in the IR spectrum of electrochemically reduced **1** (Fig. 2). Hence, we suppose that reaction (*2*) plays either minor role under our experimental conditions, or more likely not at all. Possible traces of protons in the solvent or in the supporting electrolyte may more likely attack coordinated CO forming an unstable formyl complex[22]. The higher charge consumption during the exhaustive electrolysis could also be due to close proximity of cymantrene reduction and the solvent decomposition. Under such circumstances the cymantrene intermediates may catalyze the solvent decomposition.

Reactions (*1*) and (*2*) are not the only decomposition routes of the primary reduction product. It is known that photolytically formed dicarbonyl **3**, having unsaturated coordination sphere, reacts with **1** to produce a dimer $[Mn_2(CO)_5(\eta^5\text{-}Cp)_2]$ (**6**) in which the metal–metal bond has been formed[23]. The presence of $\mathbf{6}^{-}$, at least as an intermediate, in the overall reaction sequence should be considered. Furthermore, organometallic π-complex radicals undergo in many cases a change of hapticity of the bond to the metal, followed by subsequent dimerization. While π-complexes having 17e metal configuration seem to favor dimerization *via* metal–metal bond formation, 19e forms prefer a coupling site localized on ligands[24,25] (Eq. (*3*)).

$$2\ \underset{\mathbf{1}^-}{[Mn(CO)_3(\eta^5\text{-}Cp)]^-} \rightarrow \underset{\mathbf{7}^{2-}}{[(CO)_3Mn(\eta^4\text{-}Cp)\text{–}(\eta^4\text{-}Cp)Mn(CO)_3]^{2-}} \qquad (3)$$

The formation of one (or both) of these dimers is supported by the observation of anodic peak C′ at –1.14 V, *i.e.* at the same potential as voltammetric peaks of other related manganese dimers[26]. The dimerization yielding **6** is favored by CO dissociation leading to the formation of $\mathbf{3}^-$. On the contrary, the atmosphere of CO, which suppresses the CO ligand dissociation, forces the reduced $\mathbf{1}^-$ to stabilize by means of Cp slippage or Cp elimination. In both cases, the formation of larger molecules may promote their adsorption on the electrode surface. Indeed, the peak C′ at –1.14 V is accompanied by a small peak at –1.05 V, which has symmetrical shape typical for adsorption post-peaks. Trapezoidal voltammetry, using product accumulation at –2.6 V, accentuates adsorption effects and yields a large symmetrical adsorption maximum at the potential of C′. Long accumulation may lead to irregular current maxima in the potential region of the peak C′. Adsorption phenomena were observed during the exhaustive electrolysis, described below. This confirms the formation of a highly surface active product(s) and indirectly points to the formation of larger molecules. Since the presence of free CO increases the anodic voltammetric peak C′, it could be assigned to the formation of dimer **7**. *In situ* IR spectra show a reduction product with shifted CO-stretching frequencies (ν(CO) = 1 776 and 1 731 cm^{-1}). Decreased π-acceptor properties of Cp–Cp ligand in η^4-bonding mode will result in a higher electron density on metal centres of $\mathbf{7}^{2-}$, resulting in lower CO frequencies. However, reoxidation of completely reduced **1** in the spectroelectrochemical cell only results in the 50% recovery of **1**, which is an argument for interpretation of peak C′ as oxidation of dimer **6**. The elucidation which dimer plays the dominating role remains still an open question. The identification of species in electrolyzed solution is problematic due to their instability[23,25].

Reduction of **1** by strong reducing agents like sodium amalgam[21] leads to the elimination of Cp^- ligand and formation of $[Mn(CO)_5]^-$ ($\mathbf{8}^-$). Indeed, a substantial amount of $\mathbf{8}^-$ is produced also by electrochemical reduction of **1**. This is evidenced by the presence of spectral bands at 1 895 and 1 865 cm^{-1} during electrolysis of both **1** and $[Mn_2(CO)_{10}]$ (see Fig. 2). Another argument for the formation of $\mathbf{8}^-$ follows from the comparison with voltammetry of $[Mn_2(CO)_{10}]$ shown in Fig. 3.

Since it is known that the reduction of $[Mn_2(CO)_{10}]$ yields $\mathbf{8}^-$, the anodic peak D′ at –0.1 V in Fig. 3 unambiguously corresponds to $\mathbf{8}^-$. Additional CO molecules required for the formation of $\mathbf{8}^-$ are generated *in situ* as a result of the ligand dissociation process given in Eq. (*1*).

The preparation and identification of reduction products was attempted. However, the exhaustive electrolysis at the potential –2.4 V proceeds in an anomalous way; the electrolytic current increases for about 20% of the electrolysis time and only then it decays. This suggests the participation of a catalytic process, initiated by the electron transfer. The electrolytic current reaches the level of the background current after consumption of about two electrons per molecule, which contradicts the observation of one-electron reduction in voltammetry or polarography. It is noteworthy that preparative electrolysis produces a highly adsorbable product. The mechanically mixed working mercury-pool electrode decomposes to a large amount of droplets, which remain separated. The reduced solution is dark red, highly air-sensitive and the original color fades rapidly. Despite all precautions, red color turned dark brown within few minutes and a precipitate was usually formed before a voltammogram of a red product could be recorded. Due to fast decomposition reactions, the identification methods and the voltammetry of an electrolyzed sample (anodic waves at –0.3 and –0.5 V) seems to have little relevance to interpretation of primary redox processes observed in voltammetry.

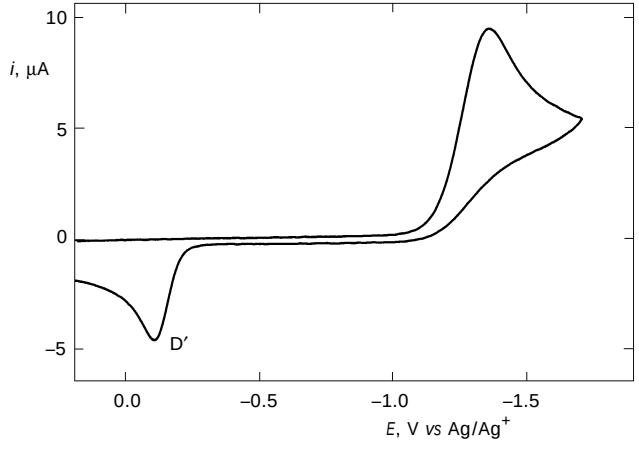

FIG. 3
Cyclic voltammetry of 1 mM $[Mn_2(CO)_{10}]$ and 0.1 M $TBAPF_6$ in acetonitrile at the scan rate 0.5 V s^{-1}

*Reduction of Cymantrene Methyl Carboximidate **2***

The cyclic voltammogram of **2** in acetonitrile is shown in Fig. 4a. The main reduction wave A is located at a potential –2.10 V (less negative by 0.3 V than in the case of **1**). Peak A is followed by another reduction peak S at –2.7 V that is close to solution decomposition and originates from redox activity of the substituent on Cp. This result is in agreement with the behavior of other ring-substituted cymantrene complexes[18]. Peak A indicates

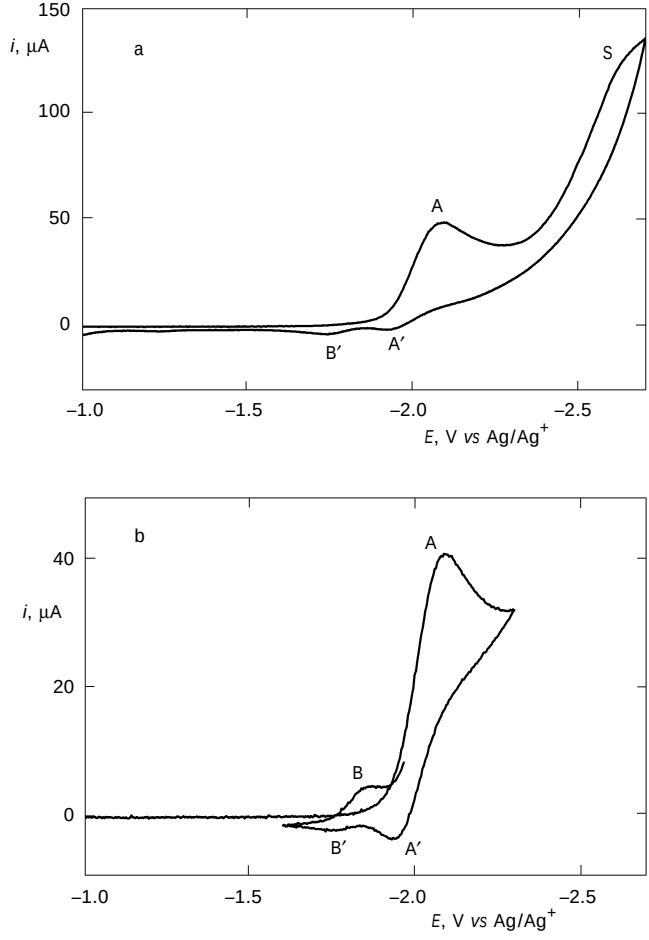

FIG. 4
Cyclic voltammetry of 1.85 mM $[Mn(CO)_3(\eta^5\text{-}C_5H_4C(NH)OMe)]$ (**2**) and 0.1 M $TBAPF_6$ in acetonitrile at scan rate 0.5 V s^{-1}. The vertex potentials were: a –2.7 V, b –2.3 and –1.4 V

higher chemical reversibility then the reduction of **1**, since its anodic branch shows the presence of an oxidation current A′. The consecutive reactions are obviously much slower than in the case of reduced **1**. Chemical consecutive reactions are eliminated at the scan rate 4 V s^{-1} (not shown) and the reduction peak A has its anodic counterpart A′. Chemical reversibility of the redox pair B/B′ at –1.8 V is clearly seen in Fig. 4b, where the second switching potential was set to –1.4 V.

Trapezoidal voltammetry with accumulation at –2.2 V leads to decreased peak A′ and increased product peak B′, as expected by analogy with **1**. Besides that, a small peak at –0.1 V, ascribed above to $\mathbf{8}^-$, becomes discernable. The accumulation also points to participation of decomposition processes similar to those seen during the exhaustive electrolysis. This is evidenced by a small anodic peak at –0.58 V. Saturation of a solution of **2** with gaseous CO increases the reversibility of peak A, as can be inferred from much larger anodic peak A′. Voltammetric peaks of the redox couple B/B′ diminish in the presence of CO, as expected. Trapezoidal voltammetry with accumulation at –2.2 V in CO-saturated solution provides expected effects: decreased A′, increased B′, more intense anodic peak of $\mathbf{8}^-$ at –0.1 V, as well as that around –0.5 V. Subsequent passing argon through the solution restores a lower degree of reversibility of the cathodic process A. When the second cycle of the voltammetric scan is recorded, peak A′ considerably increases. This suggests that during the reduction process free CO was generated in the pre-electrode layer.

FTIR spectra recorded during the potential scan (Fig. 5) show noticeable differences as compared to spectra obtained for **1**; namely, the formation of a dimer is not observed for **2**.

This is evidenced by the absence of corresponding IR bands at 1 776 and 1 731 cm^{-1}, as well as by the absence of the corresponding peak C′ in the voltammetric response. Higher stability of the primary reduction intermediate to dimerization can be explained by the possible equilibrium (Scheme 2)

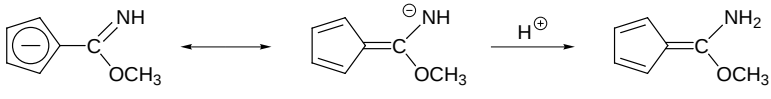

SCHEME 2

that prevents bond formation between two substituted Cp ligands. The main product of the first reduction exhibits two CO-stretching bands at 1 936 and 1 850 cm^{-1} in IR spectrum. This indicates, together with voltammetric results, that the elimination of CO ligand is the prevailing

process forming more stable 17e complex $[Mn(CO)_2(\eta^5\text{-}CpC(NH)OMe)]^-$ from the primary reduction product $\mathbf{2}^-$. The formation of detectable amount of $[Mn(CO)_5]^-$ was also confirmed as in the case of **1**. The presence of shoulders at the large wavenumber side of CO bands of **2**, observed at potentials approaching the second reduction wave, suggests the lost of a methanol molecule from the Cp substituent yielding C_5H_4–CN as a π-ligand.

CONCLUSION

The data presented here indicate that the reduction mechanism of **1** is by far more complicated than previously reported. Dessy[13] formulated the redox product as a monoanion, in agreement with voltammetry reported here. One-electron reduction yields a very unstable 19-electron intermediate, which undergoes either elimination of CO or Cp ligands. New observation in our study concerns the voltammetric pattern that includes the redox couple $\mathbf{4}^-/\mathbf{4}$, not noticed previously, which disappears if free CO is present in the solution. This points out to the participation of redox-induced chemical reaction(s) leading to the substitution of a CO ligand, most likely by the donor solvent. $[Mn(CO)_2(\eta^5\text{-}Cp)]^-$ formed by ligand dissociation is still unstable and undergoes further reactions. $[Mn(CO)_5]^-$ is identified as one of the final products. Dimerization of intermediates may

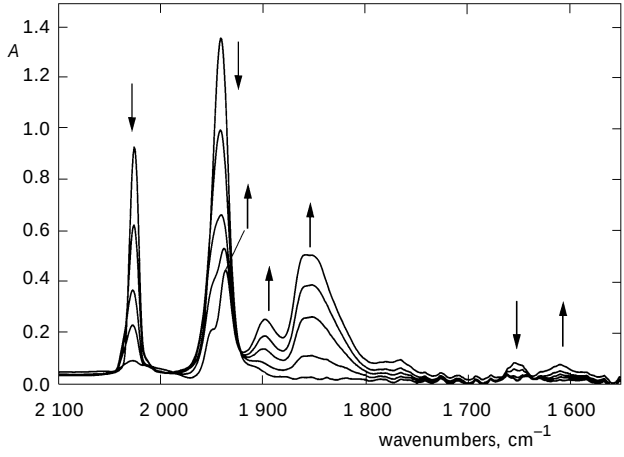

FIG. 5
FTIR spectroelectrochemistry of 5 mM $[Mn(CO)_3(\eta^5\text{-}C_5H_4C(NH)OMe)]$ (**2**) and 0.1 M $TBAPF_6$ in acetonitrile; spectra correspond to potentials –1.50, –2.0, –2.1, –2.2 and –2.3 V

involve Cp–Cp or Mn–Mn bond formation, yielding two rather different dimers. We are aware that processes reported in this study may not be a complete reaction sequence. Available experimental data comply with reaction steps in Scheme 3.

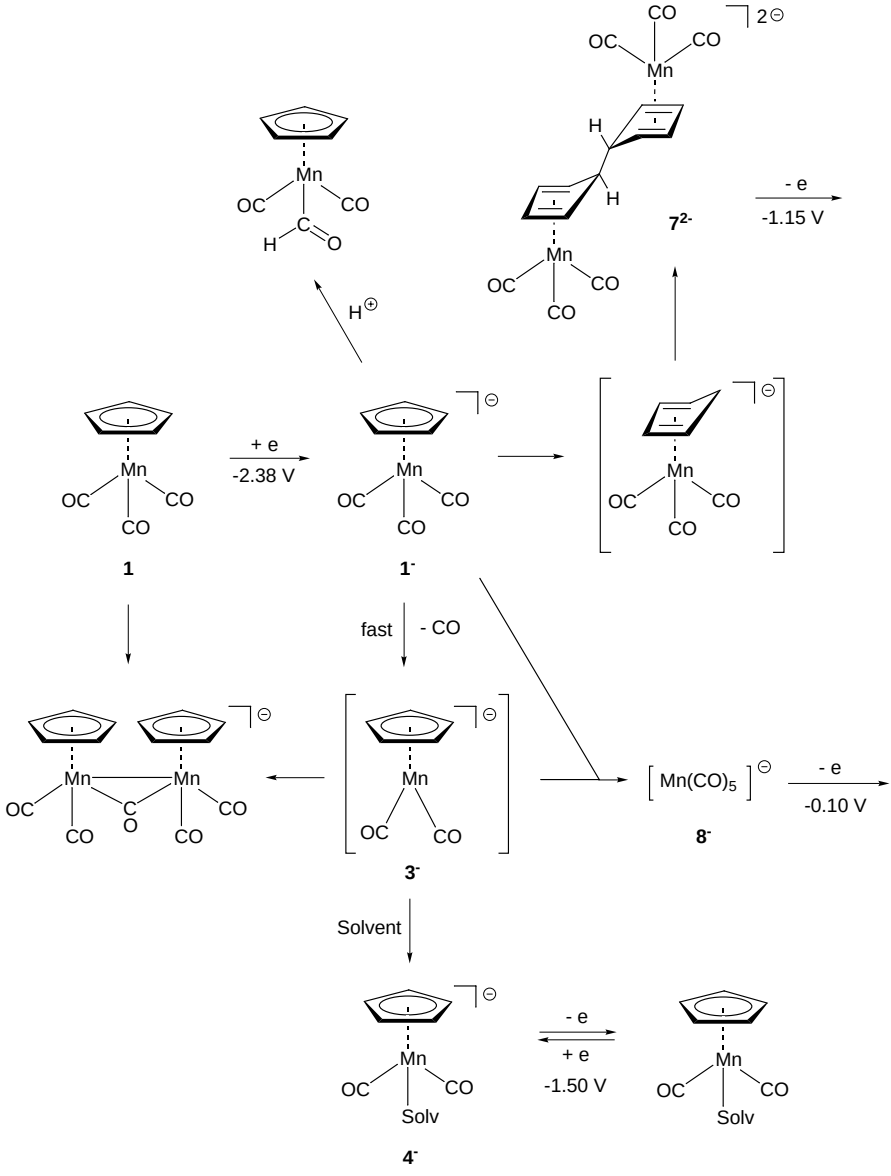

SCHEME 3

Complex **2** follows a similar reaction pattern, except the formation of a dimer. The complex sequence of EC processes seem to form an obstacle for application of **2** in the CMIA. However, we will report that **2** bound to albumin yields an electrochemical signal quite suitable for detection purposes.

The CNRS (France), the Academy of Sciences of the Czech Republic, the Grant Agency of the Czech Republic (grant No. 203/00/P007) and the Ministry of Education, Youth and Sports of the Czech Republic (grant COST D15/001/98, OC-D15.10) are gratefully acknowledged for supporting the project with exchange grants.

REFERENCES

1. Henrici-Olive G., Olive S.: *Coordination and Catalysis*. Verlag Chemie, New York 1977.
2. Darensbourg D. J.: *Adv. Organomet. Chem.* **1982**, *21*, 113.
3. Basolo F.: *Inorg. Chim. Acta* **1981**, *50*, 65.
4. Miholová D., Vlček A. A.: *J. Organomet. Chem.* **1982**, *240*, 431.
5. Hershberger J. W., Kochi J. K.: *J. Chem. Soc., Chem. Commun.* **1982**, 212.
6. Hershberger J. W., Klinger R. J., Kochi J. K.: *J. Am. Chem. Soc.* **1983**, *105*, 61.
7. Amatore C., Bayachou M., Verpeaux J.-N., Pospíšil L., Fiedler J.: *J. Electronanal. Chem.* **1995**, *387*, 101.
8. Bond A. M., Colton R.: *Coord. Chem. Rev.* **1997**, *166*, 161.
9. Salmain M., Vessieres A., Brossier P., Butler I. S., Jaouen G.: *J. Immunol. Methods* **1992**, *148*, 65.
10. Varenne A., Vessieres A., Salmain M., Brossier P., Jaouen G.: *J. Immunol. Methods* **1995**, *186*, 195.
11. Vessieres A., Salmain M., Brossier P., Jaouen G.: *J. Pharm. Biomed. Anal.* **1999**, *21*, 625.
12. Osella D., Gambino O., Fiedler J., Pospíšil L., El Amouri H., Le Brasc J., Vichard D., Gruselle M., Jaouen G.: *Inorg. Chim. Acta* **1996**, *50*, 379.
13. Dessy R. E., Stary F. E., King R. B., Hohman F.: *J. Am. Chem. Soc.* **1966**, *88*, 471.
14. Wurminghauser T., Sellmann D.: *J. Organomet. Chem.* **1980**, *57*, 77.
15. Leong V. S., Cooper N. J.: *Organometallics* **1988**, *7*, 2080.
16. Lee S., Cooper N. J.: *J. Am. Chem. Soc.* **1991**, *113*, 716.
17. Atwood C. G., Geiger W. E., Bitterwolf T. E.: *J. Electroanal. Chem.* **1995**, *397*, 279.
18. Sawtelle S. M., Johmston R. F., Cook C. C.: *Inorg. Chim. Acta* **1994**, *221*, 85.
19. Blanalt S., Salmain M., Malezieux B., Jaouen G.: *Tetrahedron Lett.* **1996**, *37*, 6561.
20. Yang P. F., Yang G. K.: *J. Am. Chem. Soc.* **1992**, *114*, 6937.
21. Wilkinson G., Stone F. G., Abel E. W. (Eds): *Comprehensive Organometallic Chemistry*, Vol. 4, p. 4. Pergamon Press, Oxford 1982.
22. Gladysz J. A.: *Adv. Organomet. Chem.* **1982**, *2*, 1.
23. Creaven B. S., Dixon A. J., Kelly J. M., Long C., Poliakoff M.: *Organometallics* **1987**, *6*, 2600.
24. Geiger W. E., Gennett T., Lane G. A., Salzer A., Rheingold A. L.: *Organometallics* **1986**, *5*, 1353.
25. Wadepohl H., Gebert S., Prizkow H., Osella D., Nervi C., Fiedler J.: *Eur. J. Inorg. Chem.* **2000**, 1833.
26. Lemoin P., Gross M.: *J. Organomet. Chem.* **1977**, *133*, 193.